Chapter 6

Model Neurons II: Conductances and Morphology

6.1 Levels of Neuron Modeling

In modeling neurons, we must deal with two types of complexity; the intricate interplay of active conductances that makes neuronal dynamics so rich and interesting, and the elaborate morphology that allows neurons to receive and integrate inputs from so many other neurons. The first part of this chapter extends the material presented in chapter 5, by examining single-compartment models with a wider variety of voltage-dependent conductances, and hence a wider range of dynamic behaviors, than the Hodgkin-Huxley model. In the second part of the chapter, we introduce methods that allow us to study the effects of morphology on the electrical characteristics of neurons. An analytic approach known as cable theory is presented first, followed by a discussion of multi-compartment models that permit numerical simulation of complex neuronal structures.

Model neurons range from greatly simplified caricatures to highly detailed descriptions involving thousands of differential equations. Choosing the most appropriate level of modeling for a given research problem requires a careful assessment of the experimental information available and a clear understanding of the research goals. Oversimplified models can, of course, give misleading results, but excessively detailed models can obscure interesting results beneath inessential and unconstrained complexity.

6.2 Conductance-Based Models

conductance-based model

The electrical properties of neurons arise from membrane conductances with a wide variety of properties. The basic formalism developed by Hodgkin and Huxley to describe the Na^+ and K^+ conductances responsible for generating action potentials (discussed in chapter 5) is also used to represent most of the additional conductances encountered in neuron modeling. Models that treat these aspects of ionic conductances, known as conductance-based models, can reproduce the rich and complex dynamics of real neurons quite accurately. In this chapter, we discuss both single- and multi-compartment conductance-based models, beginning with the single-compartment case.

To review from chapter 5, the membrane potential of a single-compartment neuron model, V, is determined by integrating the equation

$$c_m \frac{dV}{dt} = -i_m + \frac{I_e}{A}. \tag{6.1}$$

with I_e the electrode current, A the membrane surface area of the cell, and i_m the membrane current. In the following subsections, we present expressions for the membrane current in terms of the reversal potentials, maximal conductance parameters, and gating variables of the different conductances of the models being considered. The gating variables and V comprise the dynamic variables of the model. All the gating variables are determined by equations of the form

$$\tau_z(V) \frac{dz}{dt} = z_\infty(V) - z \tag{6.2}$$

where we have used the letter z to denote a generic gating variable. The functions $\tau_z(V)$ and $z_\infty(V)$ are determined from experimental data. For some conductances, these are written in terms of the open and closing rates $\alpha_z(V)$ and $\beta_z(V)$ (see chapter 5) as

$$\tau_z(V) = \frac{1}{\alpha_z(V) + \beta_z(V)} \quad \text{and} \quad z_\infty(V) = \frac{\alpha_z(V)}{\alpha_z(V) + \beta_z(V)}. \tag{6.3}$$

We have written $\tau_z(V)$ and $z_\infty(V)$ as functions of the membrane potential, but for Ca^{2+}-dependent currents they also depend on the internal Ca^{2+} concentration. We call the $\alpha_z(V)$, $\beta_z(V)$, $\tau_z(V)$, and $z_\infty(V)$ collectively gating functions. A method for numerically integrating equations 6.1 and 6.2 is described in the appendices of chapter 5.

In the following subsections, some basic features of conductance-based models are presented in a sequence of examples of increasing complexity. We do this to illustrate the effects of various conductances and combinations of conductances on neuronal activity. Different cells (and even the same cell held at different resting potentials) can have quite different response properties due to their particular combinations of conductances.

Research on conductance-based models focuses on understanding how neuronal response dynamics arises from the properties of membrane and synaptic conductances, and how the characteristics of different neurons interact when they are coupled to each other in networks.

The Connor-Stevens Model

The Hodgkin-Huxley model of action potential generation, discussed in chapter 5, was developed on the basis of data from the giant axon of the squid, and we present a multi-compartment simulation of action potential propagation using this model in a later section. The Connor-Stevens model (Connor and Stevens, 1971; Connor et al. 1977) provides an alternative description of action potential generation. Like the Hodgkin-Huxley model, it contains fast Na^+, delayed-rectifier K^+, and leakage conductances. The fast $Na^+$and delayed-rectifier K^+ conductances have somewhat different properties from those of the Hodgkin-Huxley model, in particular faster kinetics, so the action potentials are briefer. In addition, the Connor-Stevens model contains an extra K^+ conductance, called the A-current, that is transient. K^+ conductances come in wide variety of different forms, and the Connor-Stevens model involves two of them.

A-type potassium current

The membrane current in the Connor-Stevens model is

$$i_{\rm m} = \overline{g}_L(V - E_{\rm L}) + \overline{g}_{\rm Na} m^3 h (V - E_{\rm Na}) + \overline{g}_K n^4 (V - E_{\rm K}) + \overline{g}_{\rm A} a^3 b (V - E_{\rm A}) \tag{6.4}$$

where $\overline{g}_{\rm L} = 0.003$ mS/mm^2 and $E_{\rm L}$ = -17 mV are the maximal conductance and reversal potential for the leak conductance, and $\overline{g}_{\rm Na} = 1.2$ mS/mm^2, $\overline{g}_{\rm K} = 0.2$ mS/mm^2, $\overline{g}_{\rm A} = 0.477$ mS/mm^2, $E_{\rm Na}$ = 55 mV, $E_{\rm K}$ = -72 mV, and $E_{\rm A}$ = -75 mV (although the A-current is carried by K^+, the model does not require $E_{\rm A} = E_{\rm K}$) and are similar parameters for the active conductances. The gating variables, m, h, n, a, and b, are determined by equations of the form 6.2 with the gating functions given in appendix A.

The fast Na^+ and delayed-rectifier K^+ conductances generate action potentials in the Connor-Stevens model just as they do in the Hodgkin-Huxley model (see chapter 5). What is the role of the additional A-current? Figure 6.1 illustrates action potential generation in the Connor-Stevens model. In the absence of an injected electrode current or synaptic input, the membrane potential of the model remains constant at a resting value of -68 mV. For a constant electrode current greater than a threshold value, the model neuron generates action potentials. Figure 6.1A shows how the firing rate of the model depends on the magnitude of the electrode current relative to the threshold value. The firing rate rises continuously from zero and then increases roughly linearly for currents over the range shown. Figure 6.1B shows an example of action potential generation for one particular value of the electrode current.

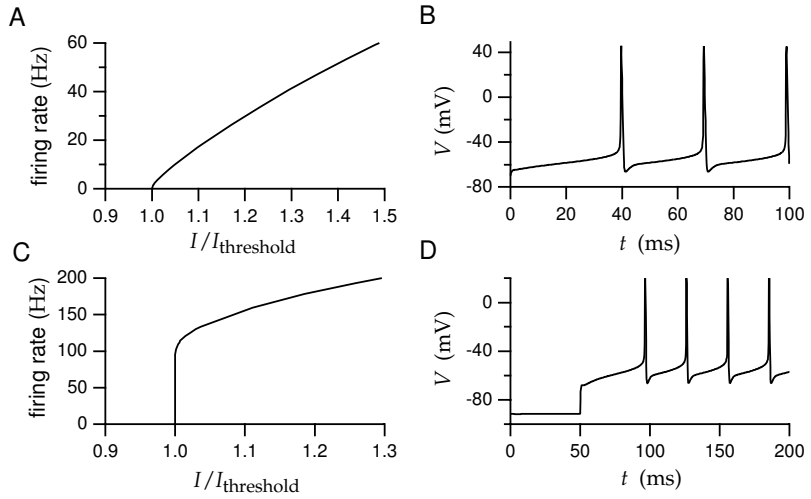

Figure 6.1: Firing of action potentials in the Connor-Stevens model. A) Firing rate as a function of electrode current. The firing rate rises continuously from zero as the current increases beyond the threshold value. B) An example of action potentials generated by constant current injection. C) Firing rate as a function of electrode current when the A-current is turned off. The firing rate now rises discontinuously from zero as the current increases beyond the threshold value. D) Delayed firing due to hyperpolarization. The neuron was held hyperpolarized for a prolonged period by injection of negative current. At $t = 50$ ms, the negative electrode current was switched to a positive value. The A-current delays the occurrence of the first action potential.

Figure 6.1C shows the firing rate as a function of electrode current for the Connor-Stevens model with the maximal conductance of the A-current set to zero. The leakage conductance and reversal potential have been adjusted to keep the resting potential and membrane resistance the same as in the original model. The firing rate is clearly much higher with the A-current turned off. This is because the deinactivation rate of the A-current limits the rise time of the membrane potential between action potentials. In addition, the transition from no firing for currents less than the threshold value to firing with suprathreshold currents is different when the A-current is eliminated. Without the A-current, the firing rate jumps discontinuously to a nonzero value rather than rising continuously. Neurons with firing rates that rise continuously from zero as a function of electrode current are called type I, and those with discontinuous jumps in their firing rates at threshold are called type II. An A-current is not the only mechanism that can produce a type I response but, as figures 6.1A and 6.1C show, it plays this role in the Connor-Stevens model. The Hodgkin-Huxley model produces a type II response.

type I, type II

Another effect of the A-current is illustrated in figure 6.1D. Here the model neuron was held hyperpolarized by negative current injection for an ex-

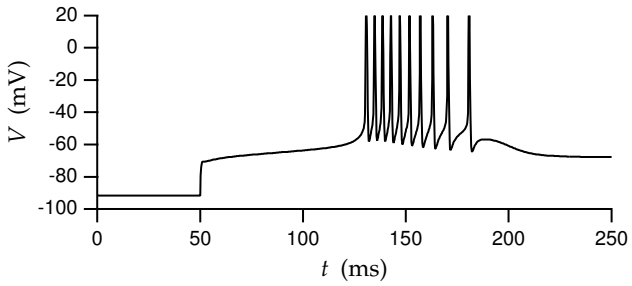

Figure 6.2: A burst of action potentials due to rebound from hyperpolarization. The model neuron was held hyperpolarized for an extended period (until the conductances came to equilibrium) by injection of constant negative electrode current. At $t = 50$ ms, the electrode current was set to zero, and a burst of Na^+ spikes was generated due to an underlying Ca^{2+} spike. The delay in the firing is caused by the presence of the A-current in the model.

tended period of time, and then the current was switched to a positive value. While the neuron was hyperpolarized, the A-current deinactivated, that is, the variable b increased toward one. When the electrode current switched sign and the neuron depolarized, the A-current first activated and then inactivated. This delayed the first spike following the change in the electrode current.

Postinhibitory Rebound and Bursting

transient Ca^{2+} conductance

The range of responses exhibited by the Connor-Stevens model neuron can be extended by including a transient Ca^{2+} conductance. The conductance we use was modeled by Huguenard and McCormick (1992) on the basis of data from thalamic relay cells. The membrane current due to the transient Ca^{2+} conductance is expressed as

$$i_{\mathrm{CaT}} = \overline{g}_{\mathrm{CaT}} M^2 H (V - E_{\mathrm{Ca}}) \tag{6.5}$$

with, for the example given here, $\overline{g}_{\mathrm{CaT}} = 13\ \mu\mathrm{S/mm}^2$ and $E_{\mathrm{Ca}} = 120$ mV. The gating variables for the transient Ca^{2+} conductance are determined from the gating functions in appendix A.

L, T, N and P type Ca^{2+} channels

Several different Ca^{2+} conductances are commonly expressed in neuronal membranes. These are categorized as L, T, N, and P types. L-type Ca^{2+} currents are persistent as far as their voltage dependence is concerned, and they activate at a relatively high threshold. They inactivate due to a Ca^{2+}-dependent rather than voltage-dependent process. T-type Ca^{2+} currents have lower activation thresholds and are transient. N- and P-type Ca^{2+} conductances have intermediate thresholds and are respectively transient and persistent. They may be responsible for the Ca^{2+} entry that causes the release of transmitter at presynaptic terminals. Entry of Ca^{2+} into a neuron

has many secondary consequences ranging from gating Ca^{2+}-dependent channels to inducing long-term modifications of synaptic conductances.

Ca^{2+} spike burst

A transient Ca^{2+} conductance acts, in many ways, like a slower version of the transient Na^+ conductance that generates action potentials. Instead of producing an action potential, a transient Ca^{2+} conductance generates a slower transient depolarization sometimes called a Ca^{2+} spike. This transient depolarization causes the neuron to fire a burst of action potentials, which are Na^+ spikes riding on the slower Ca^{2+} spike. Figure 6.2 shows such a burst and illustrates one way to produce it. In this example, the model neuron was hyperpolarized for an extended period and then released from hyperpolarization by setting the electrode current to zero. During the prolonged hyperpolarization, the transient Ca^{2+} conductance deinactivated. When the electrode current was set to zero, the resulting depolarization activated the transient Ca^{2+} conductance and generated a burst of action potentials. The burst in figure 6.2 is delayed due to the presence of the A-current in the original Connor-Stevens model, and it terminates when the Ca^{2+} conductance inactivates. Generation of action potentials in response to release from hyperpolarization is called postinhibitory rebound because, in a natural setting, the hyperpolarization would be caused by inhibitory synaptic input, not by current injection.

postinhibitory rebound

thalamic relay neuron

The transient Ca^{2+} current is an important component of models of thalamic relay neurons. These neurons exhibit different firing patterns in sleep and wakeful states. Action potentials tend to appear in bursts during sleep. Figure 6.3 shows an example of three states of activity of a model thalamic relay cell due to Wang (1994) that has, in addition to fast Na^+, delayed-rectifier K^+, and transient Ca^{2+} conductances, a hyperpolarization activated mixed-cation conductance, and a persistent Na^+ conductance. The cell is silent or fires action potentials in a regular pattern or in bursts depending on the level of current injection. In particular, injection of small amounts of negative current leads to bursting. This occurs because the hyperpolarization due to the current injection deinactivates the transient Ca^{2+} current and activates the hyperpolarization activated current. The regular firing mode of the middle plot of figure 6.3 is believed to be relevant during wakeful states when the thalamus is faithfully reporting input from the sensory periphery to the cortex.

stomatogastric ganglion

Neurons can fire action potentials either at a steady rate or in bursts even in the absence of current injection or synaptic input. Periodic bursting is a common feature of neurons in central patterns generators, which are neural circuits that produce periodic patterns of activity to drive rhythmic motor behaviors such as walking, running, or chewing. To illustrate periodic bursting, we consider a model constructed to match the activity of neurons in the crustacean stomatogastric ganglion (STG), a neuronal circuit that controls chewing and digestive rhythms in the foregut of lobsters and crabs. The model contains fast Na^+, delayed-rectifier K^+, A-type K^+, and transient Ca^{2+} conductances similar to those discussed above, although the formulae and parameters used are somewhat different. In addition,

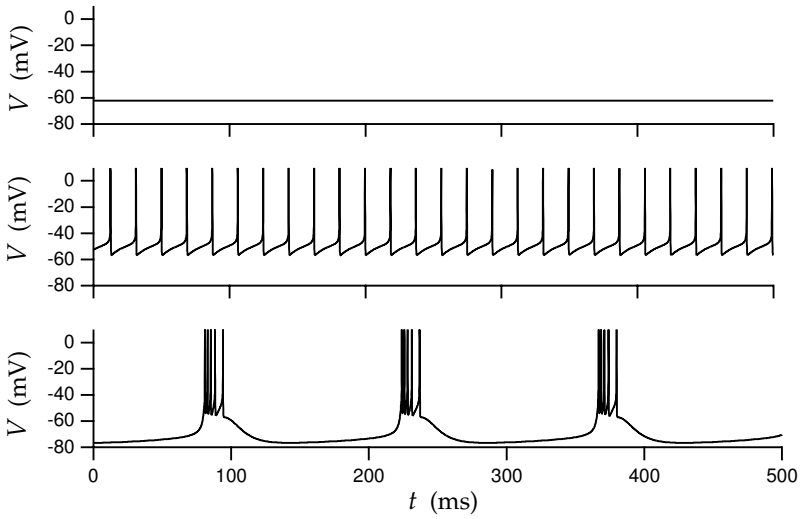

Figure 6.3: Three activity modes of a model thalamic neuron. Upper panel: with no electrode current the model is silent. Middle panel: when a positive current is injected into the model neuron, it fires action potentials in a regular periodic pattern. Lower panel: when negative current is injected into the model neuron, it fires action potentials in periodic bursts. (Adapted from Wang, 1994.)

the model has a Ca^{2+}-dependent K^+ conductance. Due to the complexity of the model, we do not provide complete descriptions of its conductances except for the Ca^{2+}-dependent K^+ conductance which plays a particularly significant role in the model.

Ca^{2+}-dependent K^+ conductance

after-hyperpolarization conductance

The repolarization of the membrane potential after an action potential is often carried out both by the delayed-rectifier K^+ conductance and by a fast Ca^{2+}-dependent K^+ conductance. Ca^{2+}-dependent K^+ conductances may be voltage dependent, but they are primarily activated by a rise in the level of intracellular Ca^{2+}. A slow Ca^{2+}-dependent K^+ conductance called the after-hyperpolarization (AHP) conductance builds up during sequences of action potentials and typically contributes to the spike-rate adaptation discussed and modeled in chapter 5.

The Ca^{2+}-dependent K^+ current in the model STG neuron is given by

$$i_{\mathrm{KCa}} = \overline{g}_{\mathrm{KCa}} c^4 (V - E_{\mathrm{K}}) \tag{6.6}$$

where c_∞ depends on both the membrane potential and the intracellular Ca^{2+} concentration, $[Ca^{2+}]$ (see appendix A). The intracellular Ca^{2+} concentration is computed in this model using a simplified description in which rises in intracellular Ca^{2+} are caused by influx through membrane Ca^{2+} channels, and Ca^{2+} removal is described by an exponential process.

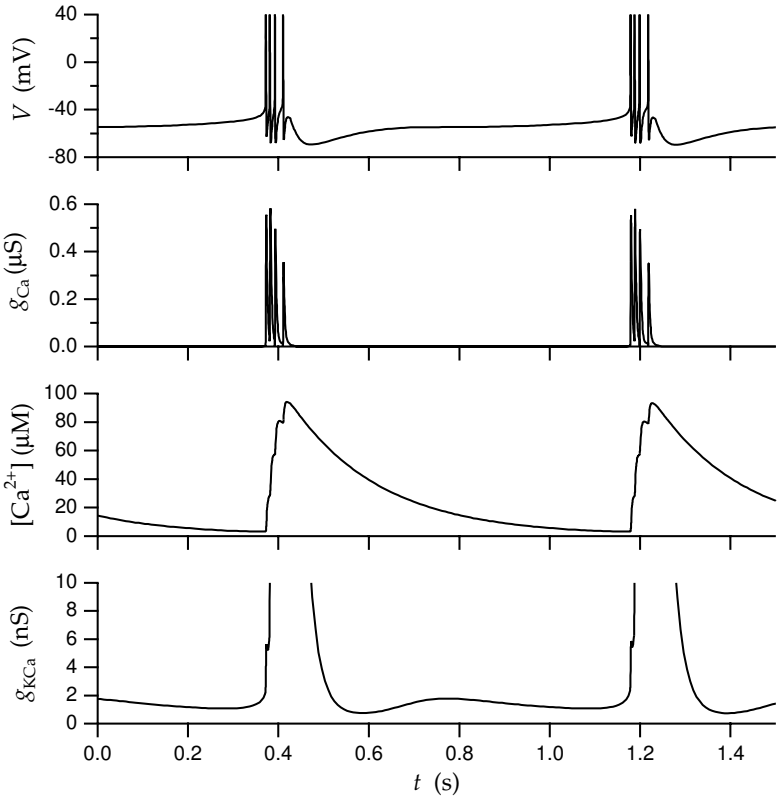

Figure 6.4: Periodic bursting in a model of a crustacean stomatogastric ganglion neuron. From the top, the panels show the membrane potential, the Ca^{2+} conductance, the intracellular Ca^{2+} concentration, and the Ca^{2+}-dependent K^+ conductance. The Ca^{2+}-dependent K^+ conductance is shown at an expanded scale so the reduction of the conductance due to the falling intracellular Ca^{2+} concentration during the interburst intervals can be seen. In this example, $\tau_{Ca} = 200$ ms. (Simulation by M. Goldman based on a variant of a model of Turrigiano et al., 1995 due to Z. Liu and M. Goldman.)

The resulting equation for the intracellular Ca^{2+} concentration, $[Ca^{2+}]$, is

$$\frac{d[Ca^{2+}]}{dt} = -\gamma i_{Ca} - \frac{[Ca^{2+}]}{\tau_{Ca}} . \tag{6.7}$$

Here i_{Ca} is the total Ca^{2+} current per unit area of membrane, τ_{Ca} is the time constant determining the rate at which intracellular Ca^{2+} is removed, and γ is a factor that converts from the electric current due to Ca^{2+} ion flow to the rate at which the Ca^{2+} ion concentration changes within the cell. Because the Ca^{2+} concentration is determined by dividing the number of Ca^{2+} ions in a cell by the total cellular volume and the Ca^{2+} influx is computed by multiplying i_{Ca} by the membrane surface area, γ is proportional

to the surface to volume ratio for the cell. It also contains a factor that converts from Coulombs per second of electrical current to moles per second of Ca^{2+} ions. This factor is $1/(zF)$ where z is the number of charges on the ion ($z = 2$ for Ca^{2+}), and F is the Faraday constant. If, as is normally the case, $[Ca^{2+}]$ is in mols/liter, γ should also contain a factor that converts the volume measure to liters, 10^6 mm^3/liter. Finally, γ must be multiplied by the additional factor that reflects fast intracellular Ca^{2+} buffering. Most of the Ca^{2+} ions that enter a neuron are rapidly bound to intracellular buffers, so only a fraction of the Ca^{2+} current through membrane channels is actually available to change the concentration $[Ca^{2+}]$ of free Ca^{2+} ions in the cell. This factor is about 1%. The minus sign in front of the γ factor in equation 6.7 is due to the definition of membrane currents as positive in the outward direction.

Figure 6.4 shows the model STG neuron firing action potentials in bursts. As in the models of figures 6.2 and 6.3, the bursts are transient Ca^{2+} spikes with action potentials riding on top of them. The Ca^{2+} current during these bursts causes a dramatic increase in the intracellular Ca^{2+} concentration. This activates the Ca^{2+}-dependent K^+ current which, along with the inactivation of the Ca^{2+} current, terminates the burst. The interburst interval is determined primarily by the time it takes for the intracellular Ca^{2+} concentration to return to a low value, which deactivates the Ca^{2+}-dependent K^+ current, allowing another burst to be generated. Although figure 6.4 shows that the conductance of the Ca^{2+}-dependent K^+ current reaches a low value immediately after each burst (due to its voltage dependence), this initial dip is too early for another burst to be generated at that point in the cycle.

The STG is a model system for investigating the effects of neuromodulators, such as amines and neuropeptides, on the activity patterns of a neural network. Neuromodulators modify neuronal and network behavior by activating, deactivating, or otherwise altering the properties of membrane and synaptic channels. Neuromodulation has a major impact on virtually all neural networks ranging from peripheral motor pattern generators like the STG to the sensory, motor, and cognitive circuits of the brain.

6.3 The Cable Equation

Single-compartment models describe the membrane potential over an entire neuron with a single variable. Membrane potentials can vary considerably over the surface of the cell membrane, especially for neurons with long and narrow processes or if we consider rapidly changing membrane potentials. Figure 6.5A shows the delay and attenuation of an action potential as it propagates from the soma out to the dendrites of a cortical pyramidal neuron. Figure 6.5B shows the delay and attenuation of an excitatory postsynaptic potential (EPSP) initiated in the dendrite by synaptic input as it spreads to the soma. Understanding these features is crucial for

determining whether and when a given synaptic input will cause a neuron to fire an action potential.

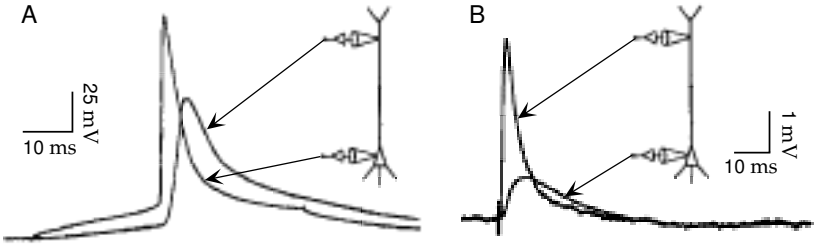

Figure 6.5: Simultaneous intracellular recordings from the soma and apical dendrite of a cortical pyramidal neuron in slice preparations. A) A pulse of current was injected into the soma of the neuron to produce the action potential seen in the somatic recording. The action potential appears delayed and with smaller amplitude in the dendritic recording. B) A set of axon fibers was stimulated producing an excitatory synaptic input. The excitatory postsynaptic potential is larger and peaks earlier in the dendrite than in the soma. Note that the scale for the potential is smaller than in A. (A adapted from Stuart and Sakmann, 1994; B adapted from Stuart and Spruston, 1998.)

cable theory

The attenuation and delay within a neuron are most severe when electrical signals travel down the long and narrow, cable-like structures of dendritic or axonal branches. For this reason, the mathematical analysis of signal propagation within neurons is called cable theory. Dendritic and axonal cables are typically narrow enough that variations of the potential in the radial or axial directions are negligible compared to longitudinal variations. Therefore, the membrane potential along a neuronal cable is expressed as a function of a single longitudinal spatial coordinate x and time, $V(x,t)$, and the basic problem is to solve for this potential.

Current flows within a neuron due to voltage gradients. In chapter 5, we discussed how the potential difference across a segment of neuronal cable is related to the longitudinal current flowing down the cable. The longitudinal resistance of a cable segment of length Δx and radius a is given by multiplying the intracellular resistivity $r_{\rm L}$ by Δx and dividing by the cross-sectional area, πa^2, so that $R_{\rm L} = r_{\rm L}\Delta x/(\pi a^2)$. The voltage drop across this length of cable, ΔV, is then related to the amount of longitudinal current flow by Ohm's law. In chapter 5, we discussed the magnitude of this current flow, but for the present purposes, we also need to define a sign convention for its direction. We define currents flowing in the direction of increasing x as positive. By this convention, the relationship between ΔV and $I_{\rm L}$ given by Ohm's law is $\Delta V = -R_{\rm L} I_{\rm L}$ or $\Delta V = -r_{\rm L}\Delta x I_{\rm L}/(\pi a^2)$. Solving this for the longitudinal current, we find $I_{\rm L} = -\pi a^2 \Delta V/(r_{\rm L}\Delta x)$. It is useful to take the limit of this expression for infinitesimally short cable segments, that is as $\Delta x \to 0$. In this limit, the ratio of ΔV to Δx becomes the derivative $\partial V/\partial x$. We use a partial derivative here, because V can also

depend on time. Thus, for at any point along a cable of radius a and intracellular resistivity r_L, the longitudinal current flowing in the direction of increasing x is

$$I_L = -\frac{\pi a^2}{r_L}\frac{\partial V}{\partial x}. \tag{6.8}$$

The membrane potential $V(x,t)$ is determined by solving a partial differential equation, the cable equation, that describes how the currents entering, leaving, and flowing within a neuron affect the rate of change of the membrane potential. To derive the cable equation, we consider the currents within the small segment shown in figure 6.6. This segment has a radius a and a short length Δx. The rate of change of the membrane potential due to currents flowing into and out of this region is determined by its capacitance. Recall from chapter 5 that the capacitance of a membrane is determined by multiplying the specific membrane capacitance c_m by the area of the membrane. The cylinder of membrane shown in figure 6.6 has a surface area of $2\pi a\Delta x$ and hence a capacitance of $2\pi a\Delta x c_m$. The amount of current needed to change the membrane potential at a rate $\partial V/\partial t$ is $2\pi a\Delta x c_m \partial V/\partial t$.

cable equation

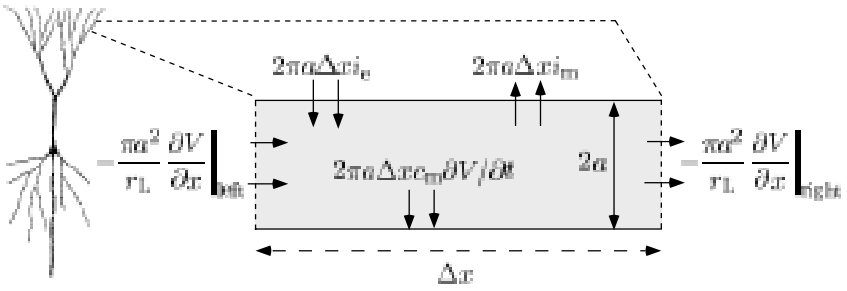

Figure 6.6: The segment of neuron used in the derivation of the cable equation. The longitudinal, membrane, and electrode currents that determine the rate of change of the membrane potential within this segment are denoted. The segment has length Δx and radius a. The expression involving the specific membrane capacitance refers to the rate at which charge builds up on the cell membrane generating changes in the membrane potential.

All of the currents that can change the membrane potential of the segment being considered are shown in figure 6.6. Current can flow longitudinally into the segment from neighboring segments, and expression 6.8 has been used in figure 6.6 to specify the longitudinal currents at both ends of the segment. Current can flow across the membrane of the segment we are considering through ion and synaptic receptor channels, or through an electrode. The contribution from ion and synaptic channels is expressed as a current per unit area of membrane i_m times the surface area of the segment, $2\pi a\Delta x$. The electrode current is not normally expressed as a current per unit area, but, for the present purposes, it is convenient to

define i_e to be the total electrode current flowing into a given region of the neuronal cable divided by the surface area of that region. The total amount of electrode current being injected into the cable segment of figure 6.6 is then $i_e 2\pi a \Delta x$. Because the electrode current is normally specified by I_e, not by a current per unit area, all the results we obtain will ultimately be re-expressed in terms of I_e. Following the standard convention, membrane and synaptic currents are defined as positive when they are outward, and electrode currents are defined as positive when they are inward.

The cable equation is derived by setting the sum of all the currents shown in figure 6.6 equal to the current needed to charge the membrane. The total longitudinal current entering the cylinder is the difference between the current flowing in on the left and that flowing out on the right. Thus,

$$2\pi a \Delta x c_m \frac{\partial V}{\partial t} = -\left(\frac{\pi a^2}{r_L}\frac{\partial V}{\partial x}\right)\Big|_{\text{left}} + \left(\frac{\pi a^2}{r_L}\frac{\partial V}{\partial x}\right)\Big|_{\text{right}} - 2\pi a \Delta x (i_m - i_e)\,. \tag{6.9}$$

Dividing both sides of this equation by $2\pi a \Delta x$, we note that the right side involves the term

$$\frac{1}{2ar_L\Delta x}\left[\left(a^2\frac{\partial V}{\partial x}\right)\Big|_{\text{right}} - \left(a^2\frac{\partial V}{\partial x}\right)\Big|_{\text{left}}\right] \rightarrow \frac{\partial}{\partial x}\left(\frac{\pi a^2}{r_L}\frac{\partial V}{\partial x}\right). \tag{6.10}$$

The arrow refers to the limit $\Delta x \rightarrow 0$, which we now take. We have moved r_L outside the derivative in this equation under the assumption that it is not a function of position. However, the factor of a^2 must remain inside the integral unless it is independent of x. Substituting the result 6.10 into 6.9, we obtain the cable equation

$$c_m \frac{\partial V}{\partial t} = \frac{1}{2ar_L}\frac{\partial}{\partial x}\left(a^2\frac{\partial V}{\partial x}\right) - i_m + i_e\,. \tag{6.11}$$

boundary conditions on the cable equation

To determine the membrane potential, equation (6.11) must be augmented by appropriate boundary conditions. The boundary conditions specify what happens to the membrane potential when the neuronal cable branches or terminates. The point at which a cable branches or equivalently where multiple cable segments join is called a node. At such a branching node, the potential must be continuous, that is, the functions $V(x,t)$ defined along each of the segments must yield the same result when evaluated at the x value corresponding to the node. In addition, charge must be conserved, which means that the sum of the longitudinal currents entering (or leaving) a node along all of its branches must be zero. According to equation 6.8, the longitudinal current entering a node is proportional to the square of the cable radius times the derivative of the potential evaluated at that point, $a^2\partial V/\partial x$. The sum of the longitudinal currents entering the node, computed by evaluating these derivatives along each cable segment at the point where they meet at the node, must be zero.

Several different boundary conditions can be imposed at the end of a terminating cable segment. A reasonable condition is that no current should flow out of the end of the cable. By equation 6.8, this means that the spatial derivative of the potential must vanish at a termination point.

Due to the complexities of neuronal membrane currents and morphologies, the cable equation is most often solved numerically using multicompartmental techniques described later in this chapter. However, it is useful to study analytic solutions of the cable equation in simple cases to get a feel for how different morphological features such as long dendritic cables, branching nodes, changes in cable radii, and cable ends affect the membrane potential.

Linear Cable Theory

Before we can solve the cable equation by any method, the membrane current i_m must be specified. We discussed models of various ion channel contributions to the membrane current in chapter 5 and earlier in this chapter. These models typically produce nonlinear expressions that are too complex to allow analytic solution of the cable equation. The analytic solutions we discuss use two rather drastic approximations; synaptic currents are ignored, and the membrane current is written as a linear function of the membrane potential. Eliminating synaptic currents requires us to examine how a neuron responds to the electrode current i_e. In some cases, electrode current can mimic the effects of a synaptic conductance, although the two are not equivalent. Nevertheless, studying responses to electrode current allows us to investigate the effects of different morphologies on membrane potentials.

Typically, a linear approximation for the membrane current is only valid if the membrane potential stays within a limited range, for example close to the resting potential of the cell. The resting potential is defined as the potential where no net current flows across the membrane. Near this potential, we approximate the membrane current per unit area as

$$i_m = (V - V_{rest})/r_m \tag{6.12}$$

where V_{rest} is the resting potential, and the factor of r_m follows from the definition of the membrane resistance. It is convenient to define v as the membrane potential relative to the resting potential, $v = V - V_{rest}$, so that $i_m = v/r_m$.

If the radii of the cable segments used to model a neuron are constant except at branches and abrupt junctions, the factor a^2 in equation 6.11 can be taken out of the derivative and combined with the prefactor $1/2ar_L$ to produce a factor $a/2r_L$ that multiplies the second spatial derivative. With this modification and use of the linear expression for the membrane current,

the cable equation for v is

$$c_m \frac{\partial v}{\partial t} = \frac{a}{2r_L} \frac{\partial^2 v}{\partial x^2} - \frac{v}{r_m} + i_e \,. \tag{6.13}$$

It is convenient to multiply this equation by r_m, turning the factor that multiplies the time derivative on the left side into the membrane time constant $\tau_m = r_m c_m$. This also changes the expression multiplying the spatial second derivative on the right side of equation 6.13 to $ar_m/2r_L$. This factor has the dimensions of length squared, and it defines a fundamental length constant for a segment of cable of radius a, the electrotonic length,

λ electrotonic length

$$\lambda = \sqrt{\frac{ar_m}{2r_L}} \,. \tag{6.14}$$

Using the values $r_m = 1\ \mathrm{M\Omega \cdot mm^2}$ and $r_L = 1\ \mathrm{k\Omega \cdot mm}$, a cable of radius $a = 2\ \mu$m has an electrotonic length of 1 mm. A segment of cable with radius a and length λ has a membrane resitance that is equal to its longitudinal resistance, as can be seen from equation 6.14,

R_λ

$$R_\lambda = \frac{r_m}{2\pi a \lambda} = \frac{r_L \lambda}{\pi a^2} \,. \tag{6.15}$$

The resistance R_λ defined by this equation is a useful quantity that enters into a number of calculations.

Expressed in terms of τ_m and λ, the cable equation becomes

$$\tau_m \frac{\partial v}{\partial t} = \lambda^2 \frac{\partial^2 v}{\partial x^2} - v + r_m i_e \,. \tag{6.16}$$

Equation 6.16 is a linear equation for v similar to the diffusion equation, and it can be solved by standard methods of mathematical analysis. The constants τ_m and λ set the scale for temporal and spatial variations in the membrane potential. For example, the membrane potential requires a time of order τ_m to settle down after a transient, and deviations in the membrane potential due to localized electrode currents decay back to zero over a length of order λ.

The membrane potential is affected both by the form of the cable equation and by the boundary conditions imposed at branching nodes and terminations. To isolate these two effects, we consider two idealized cases: an infinite cable that does not branch or terminate, and a single branching node that joins three semi-infinite cables. Of course, real neuronal cables are not infinitely long, but the solutions we find are applicable for long cables far from their ends. We determine the potential for both of these morphologies when current is injected at a single point. Because the equation we are studying is linear, the membrane potential for any other spatial distribution of electrode current can be determined by summing solutions corresponding to current injection at different points. The use of point injection to build more general solutions is a standard method of linear analysis. In this context, the solution for a point source of current injection is called a Green's function.

Green's function

An Infinite Cable

In general, solutions to the linear cable equation are functions of both position and time. However, if the current being injected is held constant, the membrane potential settles to a steady-state solution that is independent of time. Solving for this time-independent solution is easier than solving the full time-dependent equation, because the cable equation reduces to an ordinary differential equation in the static case,

$$\lambda^2 \frac{d^2v}{dx^2} = v - r_m i_e \,. \tag{6.17}$$

For the localized current injection we wish to study, i_e is zero everywhere except within a small region of size Δx around the injection site, which we take to be $x = 0$. Eventually we will let $\Delta x \to 0$. Away from the injection site, the linear cable equation is $\lambda^2 d^2v/dx^2 = v$, which has the general solution $v(x) = B_1 \exp(-x/\lambda) + B_2 \exp(x/\lambda)$ with as yet undetermined coefficients B_1 and B_2. These constant coefficients are determined by imposing boundary conditions appropriate to the particular morphology being considered. For an infinite cable, on physical grounds, we simply require that the solution does not grow without bound when $x \to \pm\infty$. This means that we must choose the solution with $B_1 = 0$ for the region $x < 0$ and the solution with $B_2 = 0$ for $x > 0$. Because the solution must be continuous at $x = 0$, we must require $B_1 = B_2 = B$, and these two solutions can be combined into a single expression $v(x) = B \exp(-|x|/\lambda)$. The remaining task is to determine B, which we do by balancing the current injected with the current that diffuses away from $x = 0$.

In the small region of size Δx around $x = 0$ where the current is injected, the full equation $\lambda^2 d^2v/dx^2 = v - r_m i_e$ must be solved. If the total amount of current injected by the electrode is I_e, the current per unit area injected into this region is $I_e/2\pi a\Delta x$. This grows without bound as $\Delta x \to 0$. The first derivative of the membrane potential $v(x) = B \exp(-|x|/\lambda)$ is discontinuous at the point $x = 0$. For small Δx, the derivative at one side of the region we are discussing (at $x = -\Delta x/2$) is approximately B/λ, while at the other side (at $x = +\Delta x/2$) it is $-B/\lambda$. In these expressions, we have used the fact that Δx is small to set $\exp(-|\Delta x|/2\lambda) \approx 1$. For small Δx, the second derivative is approximately the difference between these two first derivatives divided by Δx, which is $-2B/\lambda\Delta x$. We can ignore the term v in the cable equation within this small region, because it is not proportional to $1/\Delta x$. Substituting the expressions we have derived for the remaining terms in the equation, we find that $-2\lambda^2 B/\lambda\Delta x = -r_m I_e/2\pi a\Delta x$, which means that $B = I_e R_\lambda/2$, using R_λ from equation 6.15. Thus, the membrane potential for static current injection at the point $x = 0$ along an infinite cable is

$$v(x) = \frac{I_e R_\lambda}{2} \exp\left(-\frac{|x|}{\lambda}\right) . \tag{6.18}$$

According to this result, the membrane potential away from the site of current injection ($x = 0$) decays exponentially with length constant λ (see

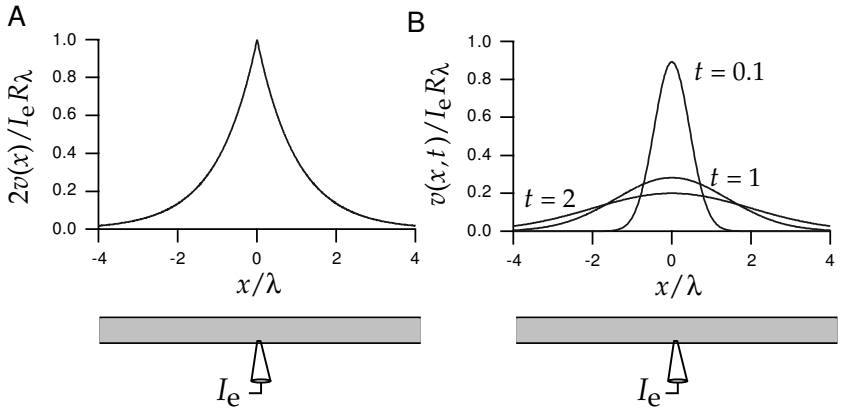

Figure 6.7: The potential for current injection at the point $x = 0$ along an infinite cable. A) Static solution for a constant electrode current. The potential decays exponentially away from the site of current injection. B) Time-dependent solution for a δ function pulse of current. The potential is described by a Gaussian function centered at the site of current injection that broadens and shrinks in amplitude over time.

figure 6.7A). The ratio of the membrane potential at the injection site to the magnitude of the injected current is called the input resistance of the cable. The value of the potential at $x = 0$ is $I_e R_\lambda/2$ indicating that the infinite cable has an input resistance of $R_\lambda/2$. Each direction of the cable acts like a resistance of R_λ and these two act in parallel to produce a total resistance half as big. Note that each semi-infinite cable extending from the point $x = 0$ has a resistance equal to a finite cable of length λ.

We now consider the membrane potential produced by an instantaneous pulse of current injected at the point $x = 0$ at the time $t = 0$. Specifically, we consider $i_e = I_e\delta(x)\delta(t)/2\pi a$. We do not derive the solution for this case (see Tuckwell, 1988, for example), but simply state the answer

$$v(x,t) = \frac{I_e R_\lambda}{\sqrt{4\pi\lambda^2 t/\tau_m}} \exp\left(-\frac{\tau_m x^2}{4\lambda^2 t}\right) \exp\left(-\frac{t}{\tau_m}\right). \qquad (6.19)$$

In this case, the spatial dependence of the potential is determined by a Gaussian, rather than an exponential function. The Gaussian is always centered around the injection site, so the potential is always largest at $x = 0$. The width of the Gaussian curve around $x = 0$ is proportional to $\lambda\sqrt{t/\tau_m}$. As expected, λ sets the scale for this spatial variation, but the width also grows as the square root of the time measured in units of τ_m. The factor $(4\pi\lambda^2 t/\tau_m)^{-1/2}$ in equation 6.19 preserves the total area under this Gaussian curve, but the additional exponential factor $\exp(-t/\tau_m)$ reduces the integrated amplitude over time. As a result, the spatial dependence of the membrane potential is described by a spreading Gaussian function with an integral that decays exponentially (figure 6.7B).

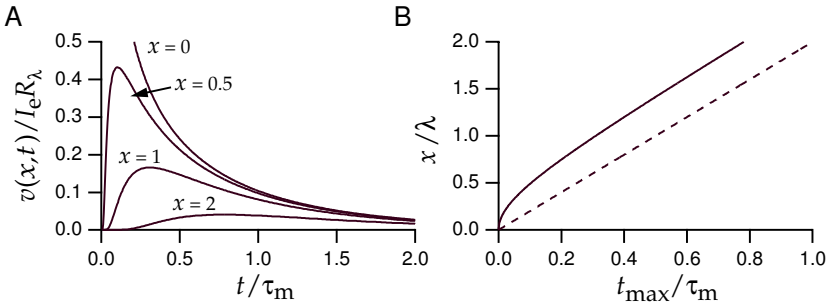

Figure 6.8: Time-dependence of the potential on an infinite cable in response to a pulse of current injected at the point $x = 0$ at time $t = 0$. A) The potential is always largest at the site of current injection. At any fixed point, it reaches its maximum value as a function of time later for measurement sites located further away from the current source. B) Movement of the temporal maximum of the potential. The solid line shows the relationship between the measurement location x, and the time t_{max} when the potential reaches its maximum value at that location. The dashed line corresponds to a constant velocity $2\lambda/\tau_m$.

Figure 6.8 illustrates the properties of the solution 6.19 plotted at various fixed positions as a function of time. Figure 6.8A shows that the membrane potential measured further from the injection site reaches its maximum value at later times. It is important to keep in mind that the membrane potential spreads out from the region $x = 0$, it does not propagate like a wave. Nevertheless, we can define a type of 'velocity' for this solution by computing the time t_{max} when the maximum of the potential occurs at a given spatial location. This is done by setting the time derivative of $v(x, t)$ in equation 6.19 to zero, giving

$$t_{max} = \frac{\tau_m}{4}\left(\sqrt{1 + 4(x/\lambda)^2} - 1\right). \tag{6.20}$$

For large x, $t_{max} \approx x\tau_m/2\lambda$ corresponding to a velocity of $2\lambda/\tau_m$. For smaller x values, the location of the maximum moves faster than this 'velocity' would imply (figure 6.8B).

An Isolated Branching Node

To illustrate the effects of branching on the membrane potential in response to a point source of current injection, we consider a single isolated junction of three semi-infinite cables as shown in the bottom panels of figure 6.9. For simplicity, we discuss the solution for static current injection at a point, but the results generalize directly to the case of time-dependent currents. We label the potentials along the three segments by v_1, v_2, and v_3, and label the distance outward from the junction point along any given segment by the coordinate x. The electrode injection site is located a distance y away from the junction along segment 2. The solution for the three

segments is then

$$\begin{aligned} v_1(x) &= p_1 I_e R_{\lambda_1} \exp(-x/\lambda_1 - y/\lambda_2) \\ v_2(x) &= \frac{I_e R_{\lambda_2}}{2}\left[\exp(-|y-x|/\lambda_2) + (2p_2 - 1)\exp(-(y+x)/\lambda_2)\right] \\ v_3(x) &= p_3 I_e R_{\lambda_3} \exp(-x/\lambda_3 - y/\lambda_2)\,, \end{aligned} \tag{6.21}$$

where, for $i = 1$, 2, and 3,

$$p_i = \frac{a_i^{3/2}}{a_1^{3/2} + a_2^{3/2} + a_3^{3/2}} \quad , \quad \lambda_i = \sqrt{\frac{r_m a_i}{2r_L}} \quad \text{, and} \quad R_{\lambda_i} = \frac{r_L \lambda_i}{\pi a_i^2}\,. \tag{6.22}$$

Note that the distances x and y appearing in the exponential functions are divided by the electrotonic length of the segment along which the potential is measured or the current is injected. This solution satisfies the cable equation, because it is constructed by combining solutions of the form 6.18. The only term that has a discontinuous first derivative within the range being considered is the first term in the expression for v_2, and this solves the cable equation at the current injection site because it is identical to 6.18. We leave it to the reader to verify that this solution satisfies the boundary conditions $v_1(0) = v_2(0) = v_3(0)$ and $\sum a_i^2 \partial v_i/\partial x = 0$.

Figure 6.9 shows the potential near a junction where a cable of radius 2 μ breaks into two thinner cables of radius 1 μ. In figure 6.9A, current is injected along the thicker cable, while in figure 6.9B it is injected along one of the thinner branches. In both cases, the site of current injection is one electrotonic length constant away from the junction. The two daughter branches have little effect on the fall-off of the potential away from the electrode site in figure 6.9A. This is because the thin branches do not represent a large current sink. The thick branch has a bigger effect on the attenuation of the potential along the thin branch receiving the electrode current in figure 6.9B. This can be seen as an asymmetry in the fall-off of the potential on either side of the electrode. Loading by the thick cable segment contributes to a quite severe attenuation between the two thin branches in figure 6.9B. Comparison of figures 6.9A and B reveals a general feature of static attenuation in a passive cable. Attenuation near the soma due to potentials arising in the periphery is typically greater than attenuation in the periphery due to potentials arising near the soma.

The Rall Model

The infinite and semi-infinite cables we have considered are clearly mathematical idealizations. We now turn to a model neuron introduced by Rall (1959, 1977) that, while still highly simplified, captures some of the important elements that affect the responses of real neurons. Most neurons receive their synaptic inputs over complex dendritic trees. The integrated effect of these inputs is usually measured from the soma, and the spike-initiation region of the axon that determines whether the neuron fires an

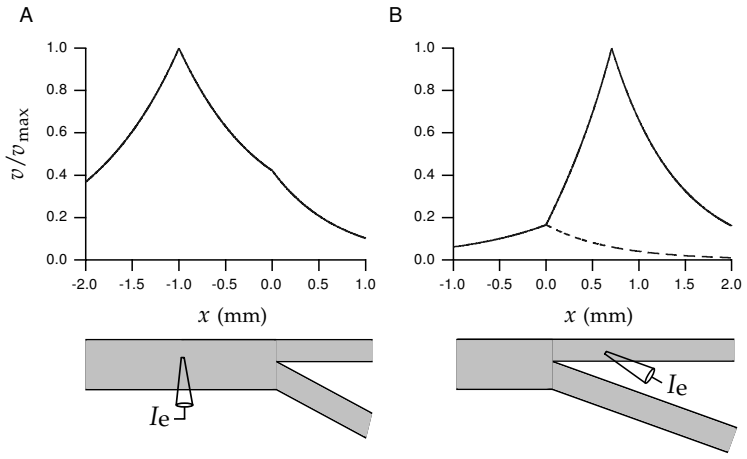

Figure 6.9: The potentials along the three branches of an isolated junction for a current injection site one electrotonic length constant away from the junction. The potential v is plotted relative to $v_{\max}$, which is v at the site of the electrode. The thick branch has a radius of 2 μ and an electrotonic length constant $\lambda = 1$ mm, and the two thin branches have radii of 1 μ and $\lambda = 2^{-1/2}$ mm. A) Current injection along the thick branch. The potentials along both of the thin branches, shown by the solid curve over the range $x > 0$, are identical. The solid curve over the range $x < 0$ shows the potential on the thick branch where current is being injected. B) Current injection along one of the thin branches. The dashed line shows the potential along the thin branch where current injection does not occur. The solid line shows the potential along the thick branch for $x < 0$ and along the thin branch receiving the injected current for $x > 0$.

action potential is typically located near the soma. In Rall's model, a compact soma region (represented by one compartment) is connected to a single equivalent cylindrical cable that replaces the entire dendritic region of the neuron (see the schematics in figures 6.10 and 6.12). The critical feature of the model is the choice of the radius and length for the equivalent cable to best match the properties of the dendritic structure being approximated.

The radius a and length L of the equivalent cable are determined by matching two important elements of the full dendritic tree. These are its average length in electrotonic units, which determines the amount of attenuation, and the total surface area, which determines the total membrane resistance and capacitance. The average electrotonic length of a dendrite is determined by considering direct paths from the soma to the terminals of the dendrite. The electrotonic lengths for these paths are constructed by measuring the distance traveled along each of the cable segments traversed in units of the electrotonic length constant for that segment. In general, the total electrotonic length measured by summing these electrotonic segment lengths depends on which terminal of the tree is used as the end point. However, an average value can be used to define an electrotonic length for the full dendritic structure. The length L of the equivalent ca-

ble is then chosen so that L/λ is equal to this average electrotonic length, where λ is the length constant for the equivalent cable. The radius of the equivalent cable, which is needed to compute λ, is determined by setting the surface area of the equivalent cable, $2\pi aL$, equal to the surface area of the full dendritic tree.

Under some restrictive circumstances the equivalent cable reproduces the effects of a full tree exactly. Among these conditions is the requirement $a_1^{3/2} = a_2^{3/2} + a_3^{3/2}$ on the radii of any three segments being joined at a nodes within the tree. Note from equation 6.22 that this conditions makes $p_1 = p_2 + p_3 = 1/2$. However, even when the so-called 3/2 law is not exact, the equivalent cable is an extremely useful and often reasonably accurate simplification.

Figures 6.10 and 6.12 depict static solutions of the Rall model for two different recording configurations expressed in the form of equivalent circuits. The equivalent circuits are an intuitive way of describing the solution of the cable equation. In figure 6.10, constant current is injected into the soma. The circuit diagram shows an arrangement of resistors that replicates the results of solving the time-independent cable equation (equation 6.17) for the purposes of voltage measurements at the soma, $v_{\rm soma}$, and at a distance x along the equivalent cable, $v(x)$. The values for these resistances (and similarly the values of R_3 and R_4 given below) are set so that the equivalent circuit reconstructs the solution of the cable equation obtained using standard methods (see for example Tuckwell, 1988). $R_{\rm soma}$ is the membrane resistance of the soma, and

$$R_1 = \frac{R_\lambda \left(\cosh\left(L/\lambda\right) - \cosh\left((L-x)/\lambda\right)\right)}{\sinh\left(L/\lambda\right)} \tag{6.23}$$

$$R_2 = \frac{R_\lambda \cosh\left((L-x)/\lambda\right)}{\sinh\left(L/\lambda\right)}\,. \tag{6.24}$$

Expressions for $v_{\rm soma}$ and $v(x)$, arising directly from the equivalent circuit using standard rules of circuit analysis (see the Mathematical Appendix), are given at the right side of figure 6.10.

The input resistance of the Rall model neuron, as measured from the soma, is determined by the somatic resistance $R_{\rm soma}$ acting in parallel with the effective resistance of the cable and is $(R_1 + R_2)R_{\rm soma}/(R_1 + R_2 + R_{\rm soma})$. The effective resistance of the cable, $R_1 + R_2 = R_\lambda/\tanh(L)$, approaches the value R_λ when $L \gg \lambda$. The effect of lengthening a cable saturates when it gets much longer than its electrotonic length. The voltage attenuation caused by the cable is defined as the ratio of the dendritic to somatic potentials, and it is given in this case by

$$\frac{v(x)}{v_{\rm soma}} = \frac{R_2}{R_1 + R_2} = \frac{\cosh\left((L-x)/\lambda\right)}{\cosh\left(L/\lambda\right)}\,. \tag{6.25}$$

This result is plotted in figure 6.11.

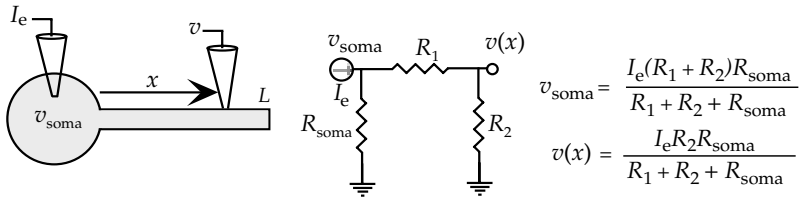

Figure 6.10: The Rall model with static current injected into the soma. The schematic at left shows the recording set up. The potential is measured at the soma and at a distance x along the equivalent cable. The central diagram is the equivalent circuit for this case, and the corresponding formulas for the somatic and dendritic voltages are given at the right. The symbols at the bottom of the resistances R_{soma} and R_2 indicate that these points are held at zero potential. R_{soma} is the membrane resistance of the soma, and R_1 and R_2 are the resistances given in equations 6.23 and 6.24.

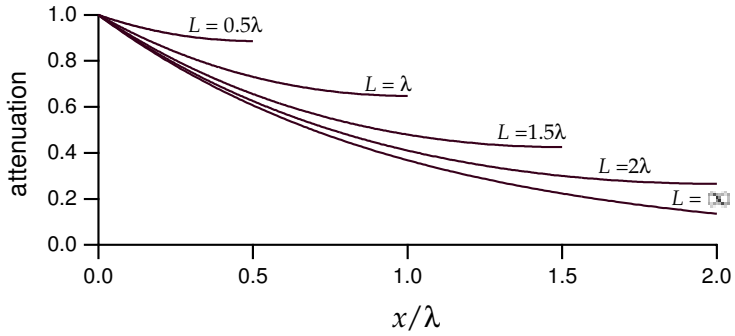

Figure 6.11: Voltage and current attenuation for the Rall model. The attenuation plotted is the ratio of the dendritic to somatic voltages for the recording setup of figure 6.10, or the ratio of the somatic current to the electrode current for the arrangement in figure 6.12. Attenuation is plotted as a function of x/λ for different equivalent cable lengths.

Figure 6.12 shows the equivalent circuit for the Rall model when current is injected at a location x along the dendritic tree and the soma is clamped at $v_{soma} = 0$ (or equivalently $V = V_{rest}$). The equivalent circuit can be used to determine the current entering the soma and the voltage at the site of current injection. In this case, the somatic resistance is irrelevant because the soma is clamped at its resting potential. The other resistances are

$$R_3 = R_\lambda \sinh(x/\lambda) \tag{6.26}$$

and

$$R_4 = \frac{R_\lambda \sinh(x/\lambda)\cosh((L-x)/\lambda)}{\cosh(L/\lambda) - \cosh((L-x)/\lambda)}. \tag{6.27}$$

The input resistance for this configuration, as measured from the dendrite, is determined by R_3 and R_4 acting in parallel and is $R_3R_4/(R_3+R_4) =$

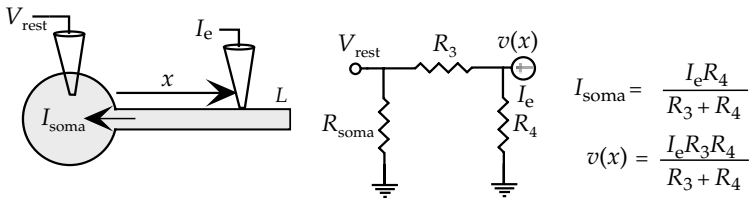

Figure 6.12: The Rall model with static current injected a distance x along the equivalent cable while the soma is clamped at its resting potential. The schematic at left shows the recording set up. The potential at the site of the current injection and the current entering the soma are measured. The central diagram is the equivalent circuit for this case, and the corresponding formulas for the somatic current and dendritic voltage are given at the right. R_{soma} is the membrane resistance of the soma, and R_3 and R_4 are the resistances given in equations 6.26 and 6.27.

$R_\lambda \sinh(x/\lambda)\cosh((L-x)/\lambda)/\cosh(L/\lambda)$. When L and x are both much larger than λ, this approaches the limiting value R_λ. The current attenuation is defined as the ratio of the somatic to electrode currents and is given by

$$\frac{I_{soma}}{I_e} = \frac{R_4}{R_3 + R_4} = \frac{\cosh((L-x)/\lambda)}{\cosh(L/\lambda)}. \tag{6.28}$$

The inward current attenuation (plotted in figure 6.11) for the recording configuration of figure 6.12 is identical to the outward voltage attenuation for figure 6.10 given by equation 6.25. Equality of the voltage attenuation measured in one direction and the current attenuation measured in the opposite direction is a general feature of linear cable theory.

The Morphoelectrotonic Transform

The membrane potential for a neuron of complex morphology is obviously much more difficult to compute than the simple cases we have considered. Fortunately, efficient numerical schemes (discussed later in this chapter) exist for generating solutions for complex cable structures. However, even when the solution is known, it is still difficult to visualize the effects of a complex morphology on the potential. Zador, Agmon-Snir, and Segev (1995; see also Tsai et al., 1994) devised a scheme for depicting the attenuation and delay of the membrane potential for complex morphologies. The voltage attenuation, as plotted in figure 6.11, is not an appropriate quantity to represent geometrically because it is not additive. Consider three points along a cable satisfying $x_1 > x_2 > x_3$. The attenuation between x_1 and x_3 is the product of the attenuation from x_1 to x_2 and from x_2 to x_3, $v(x_1)/v(x_3) = (v(x_1)/v(x_2))(v(x_2)/v(x_3))$. An additive quantity can be obtained by taking the logarithm of the attenuation, due to the identity $\ln(v(x_1)/v(x_3)) = \ln(v(x_1)/v(x_2)) + \ln(v(x_2)/v(x_3))$. The morphoelectrotonic transform is a diagram of a neuron in which the distance between

morphoelectrotonic transform